A simple and efficient super-short-scan algorithm of fan-beam reconstruction for multiple circular trajectories: solution towards the truncated data

Long Chen, Thomas Rodet, Nicolas Gac

A simple and efficient super-short-scan algorithm of Fan-beam reconstruction for multiple circular trajectories: solution towards the truncated data

Long Chen, Thomas Rodet, and Nicolas Gac

***Abstract*—The sufficiency condition of the accurate reconstruction of the region of interest (ROI) in fan-beam tomography with non-truncated data was introduced by F. Noo([1]). When the detector does not cover the whole objet, R. Clackdoyle extended this condition of the accurate reconstruction of ROI in presence of the truncated data using virtual fan-beam method (VFB) [2]. In this paper, we are interested in the image reconstruction of the whole object from truncated data, since the whole object reconstruction is always preferred even with small detector, instead of the accurate reconstruction of only a region. We propose a simple and efficient super-short-scan algorithm for multiple circular trajectories to reconstruct the whole object from truncated fan-beam projections. This algorithm is validated by simulation studies.**

I. Introduction

In fan-beam tomography, the short-scan (180° plus the fan angle) is a minimal complet data set to reconstruct the whole object [3]. This had been also hold even for the reconstruction of only a ROI [4]. A new sufficient condition of the accurate reconstruction of ROI was introduced in [1]. The ROI can be exactly reconstructed only and if only all the lines through the ROI are known. All the fan-beam projections should be non-truncated as the short scan.

When the detector is too small to cover all the object, the projection data is inevitably truncated. The accurate reconstruction of ROI is still able to be achieved in some cases with VFB in [2]. An optimal virtual fan-beam circular trajectory is found by rebinning the truncated projections to non-truncated projections. Additionally, the whole object reconstruction from the truncated data has been interesting, as in dental imaging, the panoramic view of the whole jaw from a medium detector. In this paper, we propose a simple and efficient super-short-scan (SS-scan) algorithm on twice and triple circular trajectories to achiev the reconstruction of the whole object. 'Simple' means the movement of the scanner is not complexe, and 'efficient' stands for as less fan-beam projections as possible to reconstruct the whole object. The super-short-scan projections here are not necessarily non-truncated, which are different from those in [5].

The rest of this paper is organized as follows: the proposed super-short-scans on twice and triple circular trajectories are described in section 2, we use a standard iterative least-squares method for image reconstruction in section 3. the proposed super-short-scan algorithm is evaluated by the simulation studis in section 4, and we draw the conclusion in the final section.

Long Chen is with the Laboratory of Signals and Systems, UMR8506, Université Paris-Sud-CNRS-Supélec, Gif-sur-Yvette cedex, F-91192, France

Thomas Rodet is with the Laboratory of Systems and Applications of Technologies of Information and Energy, Ecole Normale Supérieur de Cachan, Cachan cedex, F-94235, France

Nicolas Gac is with the Laboratory of Signals and Systems, UMR8506, Université Paris-Sud-CNRS-Supélec, Gif-sur-Yvette cedex, F-91192, France

II. Super-short-scans on multiple circle trajectories

In CT tomography, how to reconstruct a whole object from the truncated data is a challenge, when the detector is too small to cover all the object. Obviously, a single circular scan is able to reconstruct only a region, not the whole object. More scans are needed to achieve the whole object reconstruction. We present the proposed super-short-scans on two and three circular trajectories below.

A. Twice super-short-scans

Usually, the object support is known *a priori*. Without loss of generality, let the object support Ω be an ellipse depicted by tow semi-axis parametres (a and b, $a > b$), which is centered at origine in figure 1.(a). Two iso-centers O_1 and O_2 of scans are located symetrically to the axis Y, with distance c to the origine. The system geometry is decribed in the figure 1.(a) with distance from the X-ray source to the iso-center R, and from the source to the detector D. The length of detector is L. We have $r = L * R/D$, where r is the radius of the field of view (FOV). Obviously, r should be greater than c for the whole object reconstruction.

Intuitively, the first choice of the whole object reconstruction is to reconstruct a half ellipse from each scan. In presence of the truncated data, an optimum virtual trajectory of the X-ray is found in red solid circle using VFB ([2]), in the figure 2.(a). According to the sufficient condition in [1], two reasonable trajectories are drawn in the figure 2.(a), the scanning angle of each scan Q_1 or Q_2 is $\pi + 2 * \gamma_1$, where $\gamma_1 = \arcsin(c/R)$. As $c < r$, the angle is smaller than half of the fan angle γ_m with $\gamma_m = \arcsin(r/R)$. These tracjectories are refered to the reduced scan (R-scan). When we look at the two reduced

scans, a random pixel M in the left half of object is mesured twice in one line in the figure 2.(a). The fan-beam projections of the whole object are double from the scanning range between the lines t_1 and t_2 and between t_3 and t_4, which are the shared tangents of the object support Ω and two fileds of view (FOV) of the twice scans.

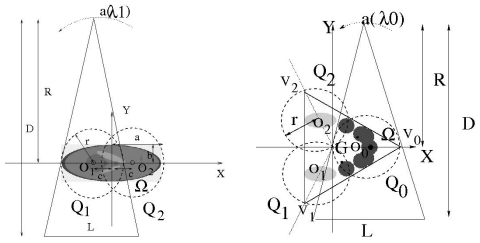

(a) Twice scans (b) Triple scans

Fig. 1: System geometries of twice scans (Q_1 and Q_2) with ellipse support of the object (a). and triple scans (Q_0, Q_1 and Q_2) for the triangular object support (b). O_i denotes the iso-center, $i = 0, 1, 2$, In (b), V_0, V_1, and V_2 are the three vertexes, their three iso-centers, O_0, O_1 and O_2, are located on the middle of the segments between the triangle gravity G and each vertex, respectively. The phantoms of Shepp-Logan (a) and simlulated jaw (b) inside Ω are given here only as exemple.

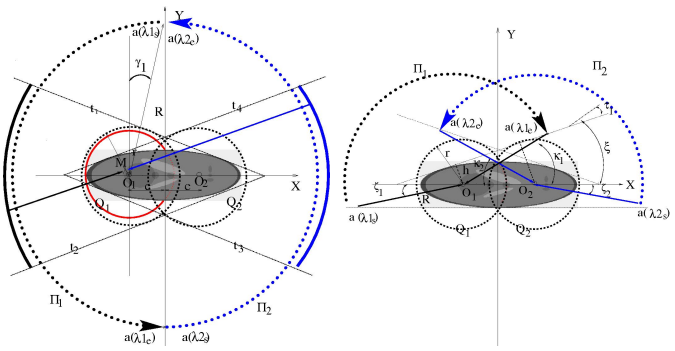

(a) R-scan (b) SS-scan

Fig. 2: Illustration of the reduced scan (a) and super-short-scan (b).

In order to reduce the data redundancy above, we propose two shorter scans refered to super-short-scans (SS-scan) in the figure 2.(b). The scanning ranges of the two super-short-scans Π_1 et Π_2 are $[\lambda 1_s \ \lambda 1_e]$ and $[\lambda 2_s \ \lambda 2_e]$ respectively. The start positions of the X-ray source $a(\lambda 1_s)$ and $a(\lambda 2_s)$ are on the tangent to the object support. In the figure 2.(b), the angle is defined positive in counterclockwise direction. $\zeta_1 = \zeta_2 = \arcsin(b/R)$, $\tau_1 = \arcsin(h/R) = \arcsin(\frac{r-2*c*sin\xi}{R})$, and $\kappa_1 = \kappa_2$,

$$\lambda 1_s = \pi + \zeta_1, \lambda 1_e = \kappa_1 = \xi + \tau_1 \quad (1)$$

$$\lambda 2_s = -\zeta_2, \lambda 2_e = \pi - \kappa_2 = \pi - (\xi + \tau_1) \quad (2)$$

where the tangent angle ξ is given by

$$tan\xi = 1/\sqrt{(\frac{r*c+\sqrt{(a^2-b^2)*(r^2-b^2)+b^2*c^2}}{r^2-b^2})^2 - 1},$$

which is derived from the solution of the tangent to the FOV of Q_1 or Q_2 and the object support function. Compared to the reduced scan, the SS scan requires less fan-beam projections. Quantitively, the reduced projection angle is given below :

$$\Delta_\Pi = \pi + 2*\gamma_1 - |\lambda 1_e - \lambda 1_s| = 2*\gamma_1 + \xi + \tau_1 - \zeta_1 \quad (3)$$

A numerical result will be given in the simulation studies, $\Delta_\Pi = 30°$.

B. *Triple super-short-scans*

When the object is much larger than the field of view of the scanner, triple scans are required for the whole object reconstruction from the truncated data. For simplification, let the object support Ω be an equilateral triangle, as in the figure 1.(b). The other parameters are defined as above.

As the object takes a great part of the FOV of each scan, no less than short-scan is able to reconstruct the part of the object inside the FOV, seperately, according to Noo's sufficient condition. A good choice is short-scan. The scanning angle of short-scan is π plus the fan angle $2*\gamma_m$. The data redundancy here is larger than in case of twice scans. We propose a triple super-short-scans to decrease

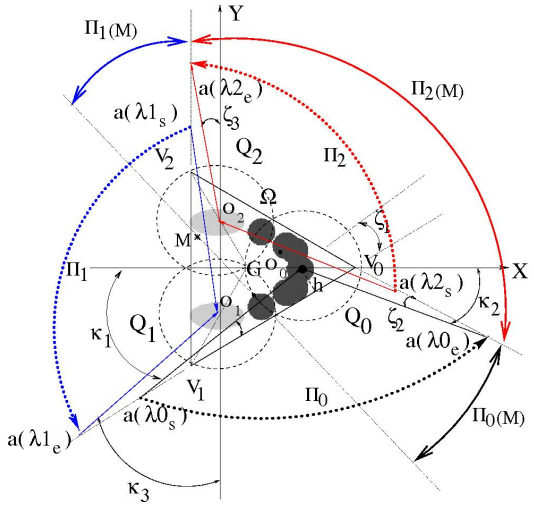

Fig. 3: Illustration of the triple super-short-scans. M is an arbitrary pixel in the object. The scanning ranges $\Pi_0(M)$, $\Pi_1(M)$ and $\Pi_2(M)$ are sufficient for the accurate reconstruction of M.

the data redundancy in the figure 3. The scanning ranges of the triple super-short-scans are Π_0, Π_1, and Π_2, where $\Pi_0 = [\lambda 0_s \ \lambda 0_e]$, $\Pi_1 = [\lambda 1_s \ \lambda 1_e]$, and $\Pi_2 = [\lambda 2_s \ \lambda 2_e]$. In the figure 3, we have the angles $\angle O_0 V_0 a(\lambda 0_s) = \angle V_2 V_0 O_0 = \pi/6$ in the equilateral triangle Ω, the start and end angular

positions of Π_0, Π_1, and Π_2 are obtained as follows:

$$\lambda 0_s = \pi + \kappa_1, \lambda 0_e = 2 * \pi - \kappa_2 \quad (4)$$

$$\lambda 1_s = \frac{\pi}{2} + \angle O_2 O_1 a(\lambda 1_s), \lambda 1_e = \frac{3\pi}{2} - \kappa_3 \quad (5)$$

$$\lambda 2_s = -\frac{\pi}{2} + \angle O_1 O_2 a(\lambda 2_s), \lambda 2_e = \frac{\pi}{2} + \zeta_3 \quad (6)$$

where $h = r * \sin(\angle O_0 V_0 a(\lambda 0_s)) = 1/2 * r$, $\zeta_1 = \zeta_2 = \zeta_3 = \angle O_2 O_1 a(\lambda 1_s) = \arcsin(h/R) = \arcsin(\frac{r}{2*R})$, $\kappa_1 = \angle O_0 V_0 a(\lambda 0_s) + \zeta_1$, $\kappa_2 = \angle V_2 V_0 O_0 - \zeta_2$, $\kappa_3 = \pi/3 - \arcsin(\frac{r}{2*R})$, and $\angle O_1 O_2 a(\lambda 2_s) = \pi/3 + \arcsin(\frac{r}{2*R})$. All the three scanning angles $|\lambda i_e - \lambda i_s|$ of Π_i are $2/3\pi$, with i=0,1,2. For the whole object reconstruction, our triple super-short scans only needs 2π fan-beam projections, which are $\pi + 6 * \gamma_m$ less than those of the triple short-scans, since each short-scan needs $\pi + 2 * \gamma_m$ fan-beam projections.

We verify the sufficient condition where every lines through the object support should be known in the figure 3: Let M be an arbitrary pixel inside the object. All the lines passing M are intersected with the three colorful solid arcs (black, red, and blue). Therefore, M is able to be reconstructed exactly. This will be validated in the results of image reconstruction from the simulated data.

III. Image reconstruction

In this paper, we consider the image reconstruction as an optimisation problem. A standard iterative least-squares (ILS) method is used for image reconstruction. The analytic methods suitable for the multiple scans are beyond this topic.

In fan-beam tomography, a forward model of data acquisition is given as follows:

$$\mathbf{g} = \mathbf{H}\mathbf{f} + \epsilon \quad (7)$$

where $\mathbf{g}$ is the mesurement vector, $\mathbf{H}$ represents the system matrix, whose element h_{ij} means the contribution of j^{th} pixel of the object on the i^{th} mesurement unit, the vector $\mathbf{f}$ describes the unknown object, and ϵ contains the detector noise and modelling errors. $\mathbf{f}$ is estimated by minimizing the criteria function $J(\mathbf{f})$ defined below:

$$J(\mathbf{f}) = 1/2\|\mathbf{g} - \mathbf{H}\mathbf{f}\|^2 \quad (8)$$

$$\hat{\mathbf{f}} = \arg\min_{\mathbf{f}} J(\mathbf{f}) \quad (9)$$

where $\|.\|^2$ is $\mathcal{L}_2$ norm. In the case of the twice scans or triple scans, $\mathbf{H}$ is rewritten as

$$\mathbf{H} = \begin{bmatrix} \mathbf{H}_1 \\ \mathbf{H}_2 \end{bmatrix}, \text{ or } \mathbf{H} = \begin{bmatrix} \mathbf{H}_0 \\ \mathbf{H}_1 \\ \mathbf{H}_2 \end{bmatrix}$$

respectively, where $\mathbf{H}_0$, $\mathbf{H}_1$, and $\mathbf{H}_2$ are the system matrices of the scans Q_0, Q_1, and Q_2, separately. In case of the twice, the gradient $\nabla J(\mathbf{f})$ and the optimal step $\hat{\alpha}$ of ILS are deducted as follows:

$$\nabla J(\mathbf{f}) = \mathbf{H}_1^T(\mathbf{H}_1\mathbf{f} - \mathbf{g}_1) + \mathbf{H}_2^T(\mathbf{H}_2\mathbf{f} - \mathbf{g}_2) \quad (10)$$

$$\hat{\alpha} = \frac{\|\nabla J(\mathbf{f})\|^2}{\nabla J(\mathbf{f})^T(\mathbf{H}_1^T\mathbf{H}_1 + \mathbf{H}_2^T\mathbf{H}_2)\nabla J(\mathbf{f})} \quad (11)$$

where $\mathbf{H}_i^T$ are the backprojections, $i = 1, 2$, $\mathbf{g}_1$ and $\mathbf{g}_2$ are the mesurements of the scans Q_1 and Q_2.

IV. Simulation studies

The proposed methods of image reconstruction of the whole object from the truncated data are evaluated by the noise-free and noisy simulated data. The geometry configuration of our CT scanner fits for dental imaging, R and D are 440 and 690 mms, there are 680 units of the detector with size of 120 μm, as a result, the achievable image size by a single circular scan is 52×52 mm^2. However, in our simulation, the support size of the standard modified Shepp-Logan (MSL) phantom (Figure 5) is 72×24 mm^2, whose attenuation coefficients are defined in matlab, and a larger simulated jaw (Figure 6) is included in an equilateral triangle support with side length 90 mm. Twice or triple circular scans are required to reconstruct the whole object. Our jaw contains 3 materials to simulate the tissu, teeth and high attenuated implants with attenuation coefficient of 0.02, 0.06 and 0.3 mm^{-1}. The fan-beam data was acquired using our ray-driven projector. To verify a stable recontruction with the proposed method, the noisy data was generated with addition of a gaussian noise in the noise-free fan-beam projections.

The images are reconstructed in 384×384 with pixel size 200 μm. The reconstructed images from the noise-free fan-beam data of MSL are presented in the left column of Figure 5. Each half of MSL is accurately reconstructed, even more the pixels inside the FOV (red dashed arc in 5.(a) and .(c)) from the reduced scan. The ILS method is able to reconstruct the MSL inside the FOV not only half of MSL from the reduced scan, as OSEM in [2]. Both twice reduced scans and twice super-short scans allow to reconstruct the whole object exactly, in the figure 5.(e) and .(g). Moreover, the scanning angle of the proposed super-short-scan decreases by 16.3%, from 184° of the reduced scan ($\pi + 2 * \gamma_1$) to 154° (equations (1) and (2)). To assure the efficacy of our proposed super-short-scan, we reduce a bit of its scanning rangs, which is refered to the SS$^-$-scan, $[\lambda 1_s - \varepsilon \ \lambda 1_e + \varepsilon]$ (clockwise) and $[\lambda 1_s + \varepsilon \ \lambda 1_e - \varepsilon]$, with a small angle ε (one or two angular steps), in the figure 2.(b). The reconstruction result is given in the figure 5.(i). The upper and centre edge of the MSL is contaminated, clearly in the profil curves of the figure 4.(a). The reconstructed images from the noisy fan-beam data are demonstrated in the right column of Figure 5. We achieve the stable restructions from all the noisy data. The image of SS$^-$-scan (Figure 5.(j)) and the profile (Figure 4.(b)) show again that the upper and center edge of MSL is not able to be reconstructed accurately decreasing the scanning range of our SS-scans.

The reconstructed images from the noise-free data and the noisy data of the simulated jaw are given in the left column of the figure 6.(a)-.(c) and in the right column 6.(d)-.(f). The accurate reconstructions of the whole jaw are achieved both on the triple short-scans (Figure 6.(a) and .(c)) and the proposed SS-scans (Figure 6.(b) and

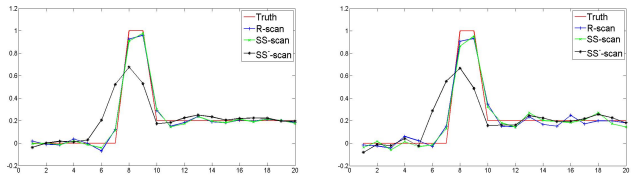

(a) Noise-free data (b) Noisy data

Fig. 4: Profiles of the reconstructed images of the whole MSL from SS$^-$-scan (a) noise-free data and (b) noisy data. The profiles are drawn along the yellow solid line in 5.(a).

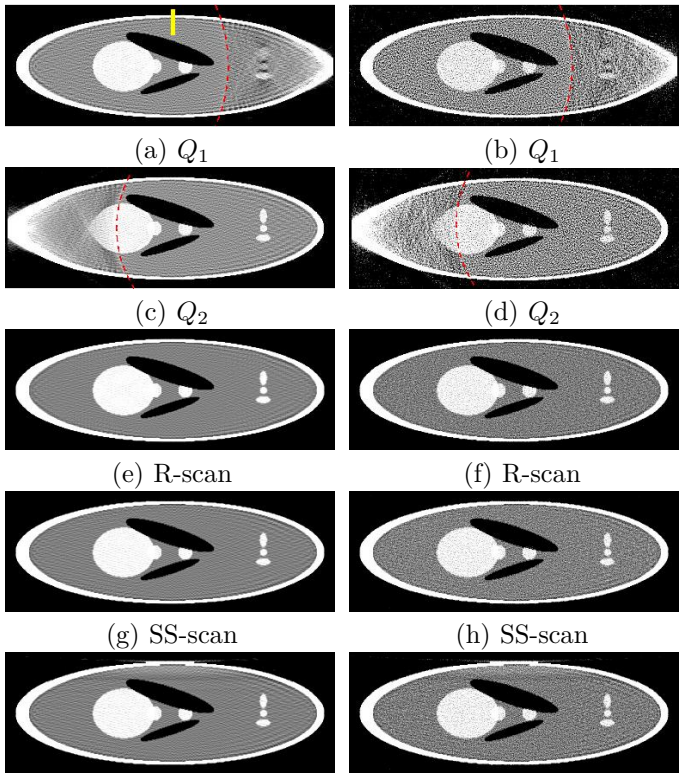

(a) Q_1 (b) Q_1

(c) Q_2 (d) Q_2

(e) R-scan (f) R-scan

(g) SS-scan (h) SS-scan

(i) SS$^-$-scan (j) SS$^-$-scan

Fig. 5: Reconstructed images from the nois-free fan-beam data (left column)and the noisy fan-beam data of MSL (right column). The display window is [0.1 0.3].

.(e)). However the proposed SS-scan requires only the fan-beam projections of 120°, which is much less than 187° (π+the fan-beam angle $2 * \gamma_m$) of the short-scan. The scanning rang using SS-scan decreases by 35.8% compared to the short-scan. Moreover, the proposed SS-scan is the minimal scan for the whole jaw reconstruction. If we reduce a few of fan-beam projections (SS$^-$-scan) with the scanning ranges $[\lambda i_s + \varepsilon\ \lambda i_e - \varepsilon], i = 0, 1, 2$ (Figure 3), some artifacts appear in the figure 6.(c) and .(f).

V. Conclusion

We propose a simple and efficient super-short-scan algorithm on twice and triple circular trajectories for the whole object image reconstruction from the truncated data. The scanning angle decreases by 16.3% in the case

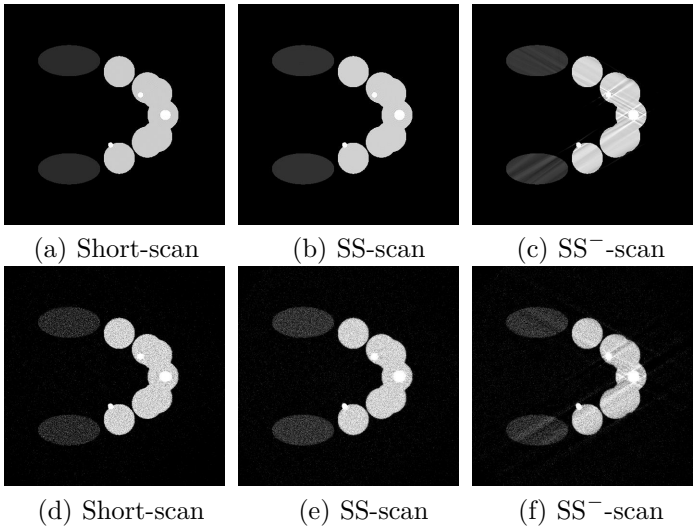

(a) Short-scan (b) SS-scan (c) SS$^-$-scan

(d) Short-scan (e) SS-scan (f) SS$^-$-scan

Fig. 6: Reconstructed images from the noise-free fan-beam data of the simulated jaw of the different acquisitions (a) short-scan, (b) SS-scan and (c) SS$^-$-scan. and from the noisy data (d) short-scan, (e) SS-scan and (f) SS$^-$-scan. The display window is [0.01 0.07].

of twice super-short scans compared to the reduced scans, and by 35.8% in the case of the proposed triple super-short scans compared to the short-scans. Our proposed super-short scans algorithms could be applied in dental imaging for a panoramic view of the whole jaw with a small detector, as well as for a fast scan and reduction of dose in other applications of CT tomography. Furthermore, these super-short scans will be easily extended in cone-beam CT tomography.

References

[1] F. Noo, M. Defrise, R. Clackdoyle, and H. Kudo, "Image reconstruction from fan-beam projections on less than a short scan," *Phys. Med. Biol.*, vol. 47, no. 02, pp. 2525–2546, 2002.

[2] R. Clackdoyle, F. Noo, J. Guo, and J.A Roberts, "Quantitative reconstruction from truncated projections in classical tomography," *IEEE Trans. Nucl. Sci.*, vol. 51, no. 5, pp. 2570–2578, 2004.

[3] D. L. Parker, "Optimal short scan convolution reconstruction for fanbeam ct," *Med. Phys.*, vol. 9, no. 2, pp. 254–257, 1982.

[4] R. Clackdoyle and M. Defrise, "Tomographic reconstruction in the 21st century," *IEEE Signal Proc. Mag.*, vol. 27, pp. 60–80, 2010.

[5] H. Kudo, and M. Defrise F. Noo, and R. Clackdoyle, "New super-short-scan algorithms for fan-beam and cone-beam reconstruction," in *Nuclear Science Symposium Conference Record, 2002 IEEE*, 2002, pp. 902 – 906.